

Application of piezoelectric cells printing on three-dimensional porous bioceramic scaffold for bone regeneration

Ming-You Shie^{1,2,3†}, Hsin-Yuan Fang^{4†}, Yen-Hong Lin^{2,5}, Alvin Kai-Xing Lee^{2,4}, Joyce Yu^{2,4}, Yi-Wen Chen^{6,7*}

¹School of Dentistry, China Medical University, Taichung City, Taiwan

²Three-dimensional Printing Medical Research Center, China Medical University Hospital, Taichung, Taiwan

³Department of Bioinformatics and Medical Engineering, Asia University, Taichung City, Taiwan

⁴School of Medicine, China Medical University, Taichung City, Taiwan

⁵The Ph.D. Program for Medical Engineering and Rehabilitation Science, China Medical University, Taichung, Taiwan

⁶Graduate Institute of Biomedical Sciences, China Medical University, Taichung City, Taiwan

⁷Three-dimensional Printing Medical Research Institute, Asia University, Taichung City, Taiwan

[†]Both authors contributed equally to this work.

Abstract: In recent years, the additive manufacture was popularly used in tissue engineering, as the various technologies for this field of research can be used. The most common method is extrusion, which is commonly used in many bioprinting applications, such as skin. In this study, we combined the two printing techniques; first, we use the extrusion technology to form the ceramic scaffold. Then, the stem cells were printed directly on the surface of the ceramic scaffold through a piezoelectric nozzle. We also evaluated the effects of polydopamine (PDA)-coated ceramic scaffolds for cell attachment after printing on the surface of the scaffold. In addition, we used fluorescein isothiocyanate to simulate the cell adhered on the scaffold surface after ejected by a piezoelectric nozzle. Finally, the attachment, growth, and differentiation behaviors of stem cell after printing on calcium silicate/polycaprolactone (CS/PCL) and PDACS/PCL surfaces were also evaluated. The PDACS/PCL scaffold is more hydrophilic than the original CS/PCL scaffold that provided for better cellular adhesion and proliferation. Moreover, the cell printing technology using the piezoelectric nozzle, the different cells can be accurately printed on the surface of the scaffold that provided and analyzed more information of the interaction between different cells on the material. We believe that this method may serve as a useful and effective approach for the regeneration of defective complex hard tissues in deep bone structures.

Keywords: Piezoelectric printing; Polydopamine; Bone tissue engineering; Calcium silicate; Polycaprolactone; Drop-on-demand

*Correspondence to: Yi-Wen Chen, Graduate Institute of Biomedical Sciences, China Medical University, Taichung 40447, Taiwan.

Tel.: 886-4-22967979 ext. 3705; Fax: 886-4-22994370; evinchen@gmail.com

Received: April 16, 2019; **Accepted:** May 23, 2019; **Published Online:** July 5, 2019

(This article belongs to the *Special Issue: Bioprinting in Asia*)

Citation: Shie M, Fang H, Lin Y, *et al.*, 2019, Application of piezoelectric cells printing on three-dimensional porous bioceramic scaffold for bone regeneration: *Int J Bioprint*, 5(2.1): 210. <http://dx.doi.org/10.18063/ijb.v5i2.1.210>

1. Introduction

Current bioprinting can be broadly classified into three categories according to their fabrication complexity: (a) Tissues with simple cellular structures

and composition such as cartilage, (b) tissues with various cells with overlapping functions such as liver or heart, and (c) tissues with extremely complex structures such as capillaries or arteries as vessels are usually

branched and closely interconnected with one another. The most commonly used bioprinting technique today is the extrusion method. There are numerous pros and cons to extrusion printing and its main disadvantage lies in its ability to print structures with fine resolutions^[1]. However, it is still widely used in research due to its low cost and simplicity and it is more commonly applied to fabricate biomimetic soft tissue instead of hard tissue such as bones. It is otherwise important to note that current technology allows us to bioprint cell-encapsulated gels which allows us to better mimic the native structures of soft tissue. However, cell encapsulated gels are usually not used for hard tissue engineering because they simply do not possess sufficient mechanical properties to match native stress demands.

In fact, there have been many mature three-dimensional (3D) printing technologies in the past, such as thermal^[2], piezoelectric^[3], and electro-hydrodynamic jetting^[4,5], but these techniques are not suitable for direct use as bioprinting. “Drop-on-demand” printing is a subtype of inkjet printing which is able to produce a tiny bead of cell-encapsulated material in a highly controlled manner. An electric current passes through a piezoelectric actuator, thus searing the nozzle to form a heated evaporated ripple and at the same moment, generating micro-droplets^[6]. It can be further sub-classified according to their various physical inducing methods such as thermal, piezoelectric, electro-hydrodynamic jetting, electrostatic bioprinting, acoustic droplet ejection, and micro-valve printing^[7]. The main disadvantage of inkjet printing lies in the fact that it has limited availability of bioink as only materials with low-viscosity of ~ 0.1 Pa·s are suitable for such printing methods^[8]. However, this technique allows us to control dictate our desired printing parameters and allow us to print structures with a printing resolution of as low as 20 μm . Furthermore, such printing technique allows us to fabricate large scales biomimetic structures as it has a fast printing speed. In addition, such printing techniques allow us to fabricate integrated multiple tissue organs or array within a narrow area. Previous reports had been made whereby heterogeneous tissues composing of triple different components were successfully fabricated using such techniques^[9]. Furthermore, other reports were made regarding fabrication of a 3D zigzag cell-encapsulated blood vessel and a 3D cell-encapsulated university logo that is of a sub-millimeter size and 13 layers thick^[10].

Bioceramics are the most widely studied biomaterial in the field of bone regeneration^[11]. According to studies, about 60% of bone substitutes found in the market are made up of biomedical-graded ceramics. Factors such as biodegradability, pore structures, porosity, permeability, and mechanical properties are critical consideration factors in the design of bone scaffolds^[12]. Once the biologically active inorganic material comes into contact

with physiological body fluids, a natural binding interface would be formed between the material and the tissues, thus creating a suitable and biomimetic platform for cellular adhesion, proliferation, differentiation, and downstream cellular activities such as bone tissue formation^[13]. At present, the most widely studied bioceramic is calcium phosphate, which has rather similar components as native bone tissues. However, it is a synthetic biomaterial, has poor degradability properties and poor osteoinductive capabilities, thus highly limiting its potential in bone tissue regeneration applications, especially so in areas of large bone defects. To improve its biological capabilities, many studies had tried adding growth factors and trace elements into bioceramics to attempt to improve its osteoinductive capabilities^[14]. These trace elements are known to be able to stimulate cell growth and to improve the bone tissue regeneration rates of calcium phosphate. Of which, the most commonly added trace element is the silicon ion (Si) and various published journals had also reported on the beneficial effects of Si on *in vivo* bone regeneration^[15,16]. In 1970, Carlisle discovered that Si ions have a positive effect on bone tissue regeneration and it was also noted that animals had an extremely high level of Si during their developmental years, thus allowing us to hypothesize that Si is closely related to bone mineralization and growth^[17]. This was further supported by the fact that the level of Si ions decreased gradually after puberty. Other than osteoinductive capabilities, another important factor in bone tissue engineering that must be considered is also angiogenic capabilities. Studies had shown that bone implants, coupled with vascular and cellular growth factor, can simultaneously induce angiogenesis. In addition, it was further reported that bioactive materials coupled with Si can induce proliferation of human umbilical vein endothelial cells (HUVECs) thus leading to increased angiogenesis^[8]. Furthermore, it had been reported that the release of Si ions by biomaterials was able to stimulate bone tissue regeneration, including cellular proliferation, differentiation, and increased expression of osteogenic genes^[18]. Due to the numerous advantages of Si ions, there were a recent hype in calcium silicate (CS) bioceramics studies, especially in the area of bone tissue engineering^[19].

Polydopamine (PDA) is a natural molecule that is rich in catechol components and amine moieties. It can be found on surfaces where mussels attach to walls in the natural world; mussels form such molecules through polymerization. PDA has also been extensively used in tissue engineering because first, it is a natural compound and second, it is found to have excellent adhesive and biocompatibility properties. In addition, it can be easily applied to biomaterials by simply soaking the material in PDA dissolved Tris buffer solution^[20]. PDA has excellent adhesive properties that allow it to be attached to nearly

all solid surfaces that it comes in contact with. This is partly due to the presence of multiple functional groups on PDA molecules. Many researchers found that PDA coating on substrate surfaces can enhance cell attachment and immobilization of numerous other compounds such as growth factors, biological peptides, extracellular matrix (ECM), and many other biomolecules^[21]. Furthermore, the desired PDA thickness could be controlled by manipulating dopamine concentration and reaction duration^[22]. For example, Rim *et al.* coated PDA onto PLLA fibers to improve the hydrophilicity of PDDA to effectively induce osteogenic differentiation and enhance calcium mineralization of human mesenchymal stem cells (hMSCs)^[23]. Chen *et al.* also coated PDA layer onto 3D printed PLA scaffold and reported that there was enhanced adhesion of human bone morphogenetic protein (rhBMP2) that led to subsequent up-regulated growth and differentiation of mouse osteoblast precursor cells to bone cells^[39]. Sun *et al.* strategically immobilized FGF-2 on PLGA scaffolds through PDA to support the proliferation of human dermal cells^[24]. In addition, Poh *et al.* modified titanium alloy with PDA coating and vascular endothelial growth factor to attempt to enhance vasculature and new bone formation^[40]. In summary, the hydrophilicity properties of PDA and its positive effects on cellular behaviors had been shown and proven to promote bone tissue growth and regeneration thus making it a suitable candidate for bone tissue engineering^[25-27].

The aim of this study is to combine two printing techniques to fabricate scaffolds with cellular deposition on its surface. Extrusion technique was used to fabricate the scaffold and a piezoelectric nozzle was used to extrude the cells onto the ceramic surface. This study would then assess for the feasibility of the intended PDA-modified CS with PCL (PDACS/PCL) scaffolds by evaluating for cellular behaviors such as cellular adhesion, proliferation, and differentiation. CS/PCL scaffold was used as the control group for this study.

2. Materials and Methods

2.1 Preparation of PDACS Powder and Scaffold

CS powders were synthesized according to our previous publication^[28]. In short, the oxide mixtures contained 70% CaO, 25% SiO₂, and 5% Al₂O₃ and were heated to 1400°C for 120 min with an ultra-high temperature furnace. Subsequently, the mixture was placed into ethyl alcohol and powdered using a centrifugal ball mill (S 100, Retsch, Hann, Germany) for 6 h. Then, the ball-milled CS powder was soaked in tris-base buffer (pH 8.5) contained dopamine (2 mg/mL, Sigma-Aldrich, St. Louis, MO, USA) and stirred for 12 h at room temperature. After the coating process for 12 h, the CS/PDA suspension

underwent filtration before being rinsed several times with 100% alcohol. The residue was then collected and quenched using an oven. The final product was PDA-modified CS (PDACS).

With the thermal pressing method, CS/PCL and PDACS/PCL matrix was made by first heating reagent grade PCL (Mw=43000–50000, Polysciences, Warrington, PA) to 150°C for 120 min. After which, CS and PDACS powders were separately suspended into 100% alcohol solutions and slowly dripped into PCL under constant stirring. The individual mixtures were then placed into an oven and heated to 100°C until the mixtures were ready for printing. For this study, the control group used was CS with PCL and the experimental group was PDACS with PCL. CS or PDACS were mixed with PCL with a mass ratio of 5:5. A precise three-axis positioning system (BioScaffolder 3.1, GeSiM, Grosserkmannsdorf, Germany) was used in this study to fabricate the desired scaffolds. The pastes were placed into syringes and were subsequently extruded through a heated steel nozzle with the following parameters: 500 kPa and 95°C. To evaluate the wettability (or hydrophilicity) of the CS/PCL and PDACS/PCL scaffold, the water contact angle was analyzed by microscope with SCA20 software (version 2.507). To measure for the water contact angle, a drop of water was dripped onto the surface of the scaffold at room temperature followed by taking an image of the water droplet. The water droplet size was controlled at 3 µL and the image was taken after 1 min, and the average value with ±standard deviation was used in this study.

2.2 FITC and ECM Adsorption

Every individual component of the bioprinter, including the piezoelectric needles, water channels, and multi-well culture dishes, and water storage tanks were sterilized with 70% alcohol and irradiated with ultraviolet light for 30 min before usage of bioprinter. In addition, the piezoelectric needles were calibrated and its parameters were adjusted using an in-built microscope lens to 90 V, 70 µs pulse width, and 100 Hz frequency. This calibration is done to ensure stability during cell dispensing so as to achieve high specificity during cellular deposition. To simulate cellular adhesion and deposition, fluorescein isothiocyanate (FITC, Sigma-Aldrich) was dissolved in Dulbecco's Modified Eagle Medium (DMEM, Invitrogen, Grand Island, NY, USA) and deposited onto the surface of the scaffolds using the following properties: Deposited at a height of 3 mm and a total of 20 droplets with a distance of 400 µm between each droplet. The scaffolds were then placed at room temperature for 0 and 30 min before being rinsed with cold phosphate-buffered saline (PBS) thrice. A BX53 Olympus fluorescence microscope was then used to observe for the status of FITC absorption on the scaffold surfaces.

In addition, ECM adsorption was performed using collagen I (Col I) and fibronectin (FN) as a model protein system and the bicinchoninic acid assay (BCA Protein Assay Kit, Thermo Scientific, Waltham, MA, USA). Briefly, CS/PCL and PDACS/PCL scaffolds were placed into the 48 well and added 500 μ L PBS (PBS, Invitrogen) contained 500 ng FN or Col I into each well at 37°C for 30 min. Then, the scaffolds were washed with PBS to remove non-adsorbed proteins and transferred to new wells. The amount of Col I and FN was quantified using the BCA kit following the manufacturer's protocol. The working reagent (500 μ L) was added into the well with the scaffolds for 15 min and transferred to new 96 well that placed into a multi-well spectrophotometer (TECAN Infinite Pro M200) at an absorbance of 562 nm. Five specimens of each scaffold were analyzed for the statistical analysis.

2.3 Cell Printing

Human Wharton's jelly mesenchymal stem cells (WJMSC) and HUVECs were purchased from the Bioresource Collection and Research Center (BCRC, Hsin-Chu, Taiwan) and cultured in DMEM supplemented with 1% penicillin/streptomycin and 10% fetal bovine serum under standard culture conditions. Cells were transformed with fluorescence to better visualize for the cytoskeleton arrangement, HUVEC and WJMSC were transformed using the CellLight Actin-RFP and CellLight Actin-GFP BacMam 2.0 system (Invitrogen) according to the supplier's instructions. The cultured cells were placed into a 96-well plate ($1 \times 10^5/100 \mu$ L) and the pathway of the piezoelectric needles was calibrated to allow it to pick up the cells and dispense them accordingly onto the struts of the scaffolds. 10 μ L of the culture solution was pipetted and dispensed on the strut of the scaffold after each layer was completed. The piezoelectric nozzle was calibrated to dispense at the height of 3 mm above the scaffold with a total of 20 droplets along the strut with a distance of 400 μ m between the droplets. The piezoelectric nozzle was calibrated to proceed to the wash station before switching to the printing of another cell line. This was to prevent any cross-contamination and to avoid any nozzle clogging. At the wash station, a strong water jet of 50 μ L/s was used to clean the inner and outer walls of the nozzle. After which, the needle would automatically dry itself before repeating the above actions. Figure 1 showed a schematic diagram of the bioprinting processes. The immunofluorescence images were taken using the BX53 Olympus fluorescence microscope.

2.4 Cell Adhesion and Proliferation

Scaffolds with WJMSC were cultured for various durations before viability evaluation with PrestoBlue® assay (Invitrogen). The above-mentioned assay detects for the level of mitochondrial activity. Briefly, 30 μ L of

PrestoBlue® solution was mixed with DMEM to a ratio of 1:10 and added to each well followed by 40 min of incubation. After which, 100 μ L from each well were transferred to a fresh 96-well ELISA plate and placed into a multi-well spectrophotometer (TECAN Infinite Pro M200) for absorbance measurement at 570 nm with a 600 nm reference wavelength. CS/PCL scaffolds were used as controls for this study. In addition, the amounts of HUVEC-RFP and WJMSC-GFP on the scaffold after cultured for different days were analyzed by LUNA-FLTM Automated Fluorescence Cell Counter (Logos Biosystems, Gyeonggi-do, South Korea). Briefly, the cells on the scaffolds were washed 3 times with PBS then digested with 0.5% trypsin-EDTA, and the culture solution was added to terminate. The cell suspension was load into the inlet of counting slide chamber and analyzed by LUNA-FLTM Cell Counter.

2.5 Osteogenesis Assay

To assess for osteogenic capabilities, alkaline phosphatase (ALP) activity levels were measured after the WJMSC were cultured with osteogenic medium (StemPro™ osteogenesis differentiation kit, Invitrogen) for 3 and 7 days. Briefly, cells were lysed with 0.2% NP-40 and left to centrifuged at 2000 rpm for 10 min. After which, the mixture was washed with PBS and ALP level was measured using p-nitrophenyl phosphate (pNPP, Sigma) with 1 M diethanolamine as a buffer. The mixture was left for 15 min at room temperature and quenched used 5N NaOH. After which, it was placed into a multi-well spectrophotometer for absorbance measurement with a wavelength of 405 nm. All studies were conducted thrice with blank cartridges used as controls.

2.6 Statistical Analysis

A one-way analysis of the variance statistical data was used to evaluate the significance of the differences between the means in the measured data. Scheffé's multiple comparison test was used to determine the significance of the deviations in the data for each specimen. In all cases, the results were considered statistically significant with $P < 0.05$.

3. Results and Discussion

3.1 Contact Angle

In the design for bone tissues scaffolds, hydrophilicity is an important factor that must be placed into consideration because it has a direct impact on influencing cellular behaviors. The contact angle between the water droplet and scaffold surface is shown in Figure 2. For the PDACS/PCL scaffolds, there was a water contact angle of 59.10° and a water contact angle of 79.85° for the CS/PCL

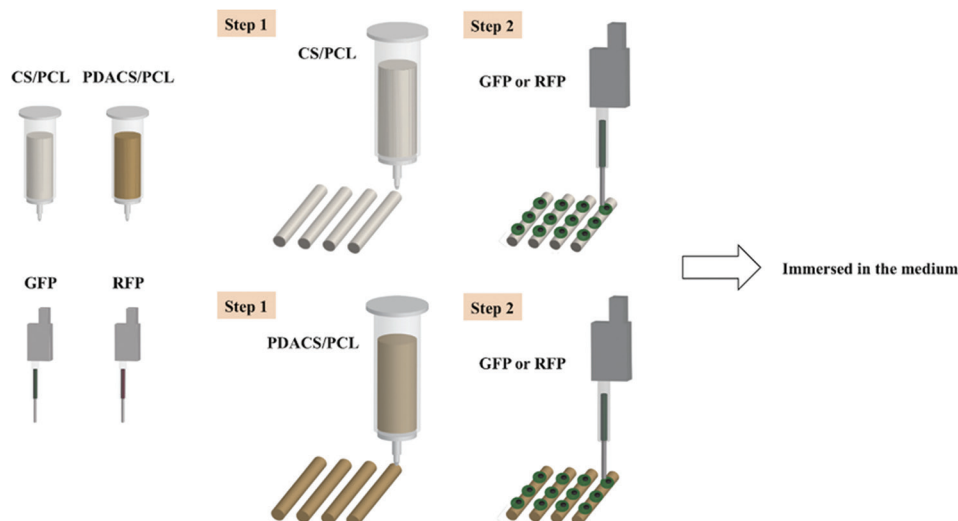


Figure 1. Schematic diagram of the bioprinting process. First, a framework was fabricated with calcium silicate/polycaprolactone (CS/PCL) and polydopamine CS/PCL composite to support scaffold stability. Second, the cells (or fluorescein isothiocyanate) were printed on the scaffold surface by the piezoelectric needle.

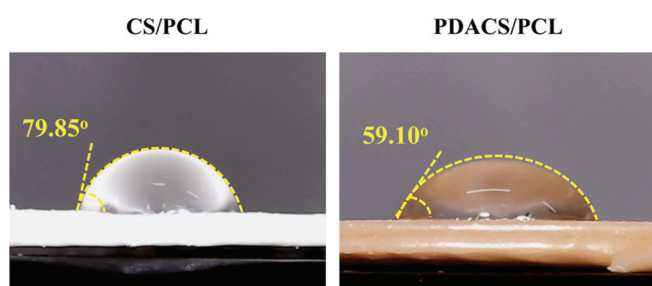


Figure 2. The water contact angle of calcium silicate/polycaprolactone (CS/PCL) and polydopamine CS/PCL scaffolds.

material. The lower contact angle on the PDACS/PCL scaffolds was hypothesized to be due to the presence of various imine and hydroxyl attachment groups on the scaffold surface^[29]. Reports had been made regarding the positive effects of hydrophilic surfaces on cellular behaviors such as adhesion and proliferation. Our above data are consistent with previously published studies in that PDA is more hydrophilic than pure PCL^[8].

3.2 FITC and ECM Adsorption

To confirm whether cells were able to adhere to the scaffold within a short amount of time, FITC adsorption was used to simulate and assess for cellular adhesion. **Figure 3A** illustrates the level of FITC adsorption on CS/PCL and PDACS/PCL scaffold surfaces after printing by the piezoelectric nozzle for 0 and 30 min. Scaffolds that had successful adsorption of FITC would display a bright homogenous green fluorescence under a fluorescence microscope. As shown in **Figure 3**, minute amounts of FITC were seen deposited on the CS/PCL scaffolds at 0 min after printing. After 30 min, there

was a slight increase in FITC adsorption as seen from the green fluorescence. However, FITC adsorption was scattered and dispersed as compared to FITC adsorption on the PDACS/PCL scaffold. On the other hand, it was worthy to note that there PDACS/PCL scaffold had increased amounts of FITC adsorption at both 0 min and 30 min as indicated by the presence of more intense fluorescence. As seen, FITC was able to be successfully adsorbed onto PDACS/PCL surfaces even at 0 min after printing. Although it was scattered and dispersed, this initial result showed that PDACS/PCL modification was able to enhance protein adsorption, which translates to enhanced cellular adhesion. Increased protein adsorption properties of scaffold surfaces were known to directly influence cellular adhesion and attachment and thus upregulating subsequent downstream cellular behaviors. At the 30 min mark, the fluorescence intensity on the PDACS/PCL scaffold was the strongest thus indicative of its protein adsorption capability as compared to CS/PCL scaffold.

Figure 3B shows the amount of Col I and FN adsorbed on CS/PCL and PDACS/PCL scaffolds. As shown in **Figure 3B**, there is a statistically significant difference ($P < 0.05$) in increased Col I concentration in the PDACS/PCL scaffold (61.56 ± 5.68) when compared to the CS/PCL scaffold (45.15 ± 5.22). Furthermore, FN concentration was no significant difference ($P > 0.05$) between these two scaffolds. The data may explain the reason of the cells adhere onto surfaces of PDACS/PCL scaffold since there tends to be a direct relationship between ECM adherence and PDA-coated of scaffolds. In our recent study, we proved that ECM such as Col I and FN preferably adsorb on the surfaces of ceramic-based

biomaterials^[30]. The results in the present study were in agreement with those of the previous studies.

3.3 Cell Adhesion and Proliferation

Figure 4A showed the quantification of cellular proliferation after 10, 30, and 60 min of incubation on both the CS/PCL and PDACS/PCL scaffolds. Immunofluorescence images of the cells are shown in Figure 4B after 3 days of culture. As compared to CS/PCL, the PDACS/PCL group had significantly higher cellular proliferation after the 20 min mark ($P < 0.05$). This result is, therefore, in good agreement with the fluorescence intensity observations, as shown in Figure 3. It is thus apparent that higher protein adsorption is directly related to the PDACS/PCL modification which could lead to enhanced cellular behaviors. The PDA nanolayer has the ability to be a bridge for covalent immobilization of growth factors and proteins^[31]. Favorable adhesion and proliferation behaviors of the stem cells on the biomaterials were very important that considered useful for bone tissue engineering application^[32]. The quantitative analysis

results of cell proliferation are provided in Figure 4B. It can be seen that the PDACS/PCL scaffolds promoted cellular proliferation to a significantly higher degree ($P < 0.05$) for all time periods. The absorbance values of WJMSC cultured on PDACS/PCL for 1, 3, and 7 days were 1.22, 1.46, and 1.33 times higher than that on CS/PCL, respectively. The morphology of cellular adhesion was also visualized using the fluorescence microscope to better understand the quality of adhesion on the various scaffolds. As seen in Figure 4C, the cells cultured on the CS/PCL scaffold displayed a clustered and rounded appearance as compared to cells cultured on the PDACS/PCL scaffold. There was not much cell spreading and extension thus indicating that the cells were not fully adhered onto the scaffold. On the other hand, cells cultured on the PDACS/PCL scaffold displayed an elongated and flattened morphology thus indicating that the cells are well spread on the surface. Various studies had also similarly demonstrated that PDA coating enhances cellular adhesion and proliferation^[33]. As cellular spreading and adhesion are indicated by sufficient interaction with substrate surfaces, this also

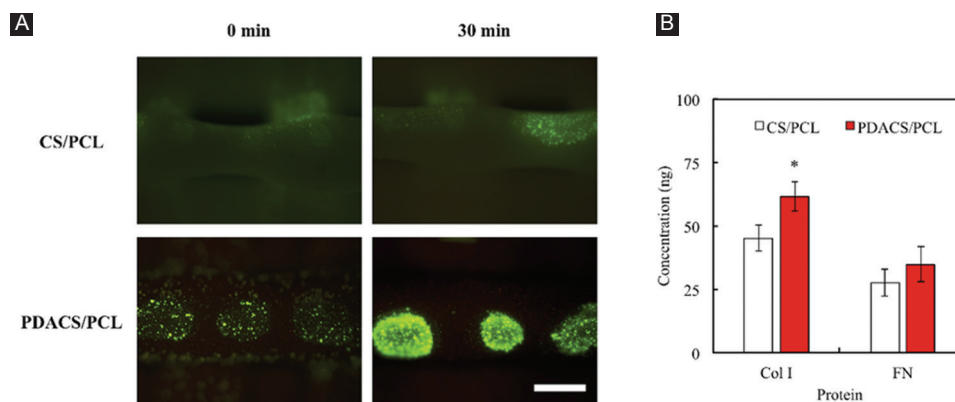


Figure 3. (A) The fluorescein isothiocyanate solution adsorbed on the calcium silicate/polycaprolactone (CS/PCL) or polydopamine CS/PCL surface after printing for 0 and 30 min. Scale bar: 400 μm . (B) The Col I and fibronectin adsorbed on scaffolds surface for 30 min. “*” indicates a significant difference ($P < 0.05$) compared to CS/PCL.

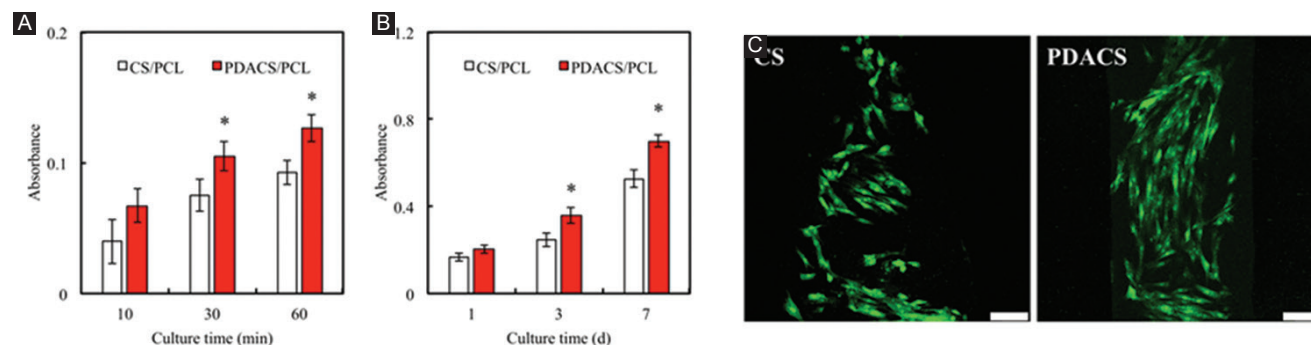


Figure 4. (A) The cell adhered and (B) proliferated on calcium silicate/polycaprolactone (CS/PCL) or polydopamine CS/PCL scaffold after printing for different time-points. “*” indicates a significant difference ($P < 0.05$) from CS/PCL. (C) The immunofluorescence of Wharton's jelly mesenchymal stem cells cultured on CS/PCL or PDACS/PCL scaffolds for 3 days. Scale bar: 100 μm .

indicates that PDACS/PCL scaffold provided improved and enhanced components for improved cellular adhesion which would lead to enhanced downstream behaviors.

3.4 Osteogenic Differentiation Ability

In addition to cell attachment and proliferation, cell differentiation is also important for new bone formation. ALP is a crucial component that is present during the pre-osteoblastic stage of stem cell differentiation^[34]. ALP activity of WJMSC printed on both the CS/PCL and PDACS/PCL scaffolds was measured after 3 and 7 days to evaluate for osteogenic capabilities which were an important factor for new bone regeneration. Figure 5 indicated that the WJMSC printed and cultured on the PDACS/PCL scaffold had significantly enhanced ALP activity as compared to CS/PCL scaffolds ($P < 0.05$). It was worthy to note that there was a statistically significant increase of 48% and 51% between the two groups after 3 and 7 days of culture, respectively. Therefore, the above results showed that PDA coating was able to enhance ALP activity, thus further indicating

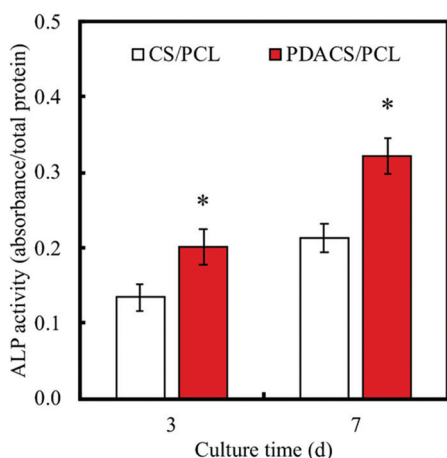


Figure 5. The alkaline phosphatase expression in the Wharton's jelly mesenchymal stem cells was cultured on calcium silicate/polycaprolactone (CS/PCL) or polydopamine CS/PCL scaffolds after printing 3 and 7 days. “*” indicates a significant difference ($P < 0.05$) compared to CS/PCL.

that PDACS/PCL scaffolds not only were able to support biocompatible but also were able to promote cellular differentiation and its downstream cellular activities^[35].

3.5 Multi Cell Printing

Cellular adhesion is the first and critical factor for subsequent downstream cellular activities. This implied that the efficiency of cellular adhesion would directly affect the extent of downstream cellular events such as proliferation and differentiation. For this study, RFP- and GFP-cells were extruded onto the scaffold in a similar manner as the FITC protein, followed by incubation and observation with fluorescence microscopy (Figure 6). As seen in Figure 6A, there was successful cellular adhesion as seen from the homogenous red and green fluorescence.

Then, the amounts of RFP-HUVEC and GFP-WJMSC after cultured for 1, 3, and 7 days were performed by a cell counter (Figure 6B). The cell proliferation of GFP-WJMSC at day-7 was significantly higher ($P < 0.05$) as compared to day-1 and day-3 onward. These results clearly indicated that the presence of the scaffold promoted WJMSC proliferation and it could be hypothesized that the hydrophilic nature of the CS scaffolds was not only favorable for cellular adhered but also led to regulated proliferation^[36]. However, the cell number of RFP-HUVEC grown on scaffold at day-3 and day-7 elicited a significant ($P < 0.05$) increase of 50% and 83% compared with day-1, respectively. In previous study, Chen et al. demonstrated the ionic products of CS-based materials dissolution stimulate cell secreted angiogenic-related proteins^[37]. Moreover, Chou *et al.* verified that the p38/MAPK pathway plays a key role in promoting the angiogenesis behavior of cell cultured with CS-based materials^[38]. Furthermore, the cells were seen to be contained in their respective extruded boundaries. This result showed that PDACS/PCL modification was able to promote cellular adhesion.

4. Conclusion

In summary, we fabricated a 3D scaffold using PDACS/PCL with raw materials and WJMSC were dispensed on

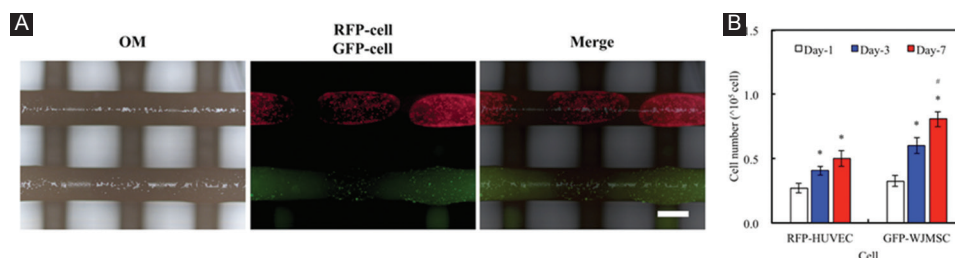


Figure 6. (A) The immunofluorescence image of RFP-cell and GFP-cell after printing on polydopamine calcium silicate/polycaprolactone scaffold surface. Scale bar: 400 μ m. (B) The amounts of RFP-human umbilical vein endothelial cells and GFP-Wharton's jelly mesenchymal stem cells cultured on scaffold for different time-point. “*” indicates a significant difference ($P < 0.05$) compared to day-1. “#” indicates a significant difference ($P < 0.05$) compared to day-3.

the materials surface through the piezoelectric needle. The PDACS/PCL scaffold was shown to be more hydrophilic than the original CS/PCL scaffold, thus allowing better cellular adhesion and proliferation. Moreover, it was shown that using the piezoelectric nozzle, different cells can be accurately printed onto the surface of the scaffold, thus allowing us to better analyze and visualize for the cell-material interactions. Therefore, we hypothesized that this mussel-inspired PDACS/PCL 3D scaffold was able to enhance cellular behaviors thus making it a potential applicant for future bone regeneration research and applications.

Acknowledgments

The authors acknowledge receipt grants from the Ministry of Science and Technology (107-2218-E-039-001 and 107-2314-B-039-070) and China Medical University Hospital grants (CRS-106-021). The authors declare that they have no conflicts of interest.

References

1. Placone JK, Engler AJ, 2018, Recent Advances in Extrusion-based 3D Printing for Biomedical Applications. *Adv Healthc Mater*, 7:1701161. DOI 10.1002/adhm.201701161.
2. Chiu YC, Fang HY, Hsu TT, *et al.*, 2017, The Characteristics of Mineral Trioxide Aggregate/Polycaprolactone 3-dimensional Scaffold with Osteogenesis Properties for Tissue Regeneration. *J Endod*, 43:923-9. DOI 10.1016/j.joen.2017.01.009.
3. Sultana A, Ghosh SK, Sencadas V, *et al.*, 2017, Human Skin Interactive Self-powered Wearable Piezoelectric Bio-skin by Electrospun Poly-l-lactic Acid Nanofibers for Non-invasive Physiological Signal Monitoring. *J Mater Chem B*, 5:7352-9. DOI 10.1039/c7tb01439b.
4. Wu Y, Wong YS, Fuh YHJ, 2017, Degradation Behaviors of Geometric Cues and Mechanical Properties in a 3D Scaffold for Tendon Repair. *J Biomed Mater Res Part A*, 105:1138-49. DOI 10.1002/jbm.a.35966.
5. Vijayavenkataraman S, Zhang S, Thaharah S, *et al.*, 2018, Electrohydrodynamic Jet 3D Printed Nerve Guide Conduits (NGCs) for Peripheral Nerve Injury Repair. *Polymers*, 10:753. DOI 10.3390/polym10070753.
6. Choi M, Heo J, Yang M, *et al.*, 2017, Inkjet Printing-based Patchable Multilayered Biomolecule-containing Nanofilms for Biomedical Applications. *ACS Biomater Sci Eng*, 3:870-4. DOI 10.1021/acsbomaterials.7b00138.
7. Yang J, Katagiri D, Mao S, *et al.*, 2016, Inkjet Printing Based Assembly of Thermoresponsive Core-shell Polymer Microcapsules for Controlled Drug Release. *J Mater Chem B*, 4:4156-63. DOI 10.1039/c6tb00424e.
8. Chen YW, Shen YF, Ho CC, *et al.*, 2018, Osteogenic and Angiogenic Potentials of the Cell-laden Hydrogel/Mussel-inspired Calcium Silicate Complex Hierarchical Porous Scaffold Fabricated by 3D Bioprinting. *Mater Sci Eng C Mater Biol Appl*, 91:679-87. DOI 10.1016/j.msec.2018.06.005.
9. Xu T, Zhao W, Zhu JM, *et al.*, 2013, Complex Heterogeneous Tissue Constructs Containing Multiple Cell Types Prepared by Inkjet Printing Technology. *Biomaterials*, 34:130-9. DOI 10.1016/j.biomaterials.2012.09.035.
10. Arai K, Iwanaga S, Toda H, *et al.*, 2011, Three-dimensional Inkjet Biofabrication Based on Designed Images. *Biofabrication*, 3:034113. DOI 10.1088/1758-5082/3/3/034113.
11. Huang KH, Chen YW, Wang CY, *et al.*, 2018, Enhanced Capability of BMP-2-loaded Mesoporous Calcium Silicate Scaffolds to Induce Odontogenic Differentiation of Human Dental Pulp Cells. *J Endod*, 44:1677-85. DOI 10.1016/j.joen.2018.08.008.
12. Hench LL, 1991, Bioceramics: From Concept to Clinic. *J Am Ceram Soc*, 74:1457-510.
13. Wang W, Yeung KWK, 2017, Bone Grafts and Biomaterials Substitutes for Bone Defect Repair: A Review. *Bioact Mater*, 2:224-47. DOI 10.1016/j.bioactmat.2017.05.007.
14. Chen YW, Hsu TT, Wang K, *et al.*, 2016, Preparation of the Fast Setting and Degrading Ca-Si-Mg Cement with both Odontogenesis and Angiogenesis Differentiation of Human Periodontal Ligament Cells. *Mater Sci Eng C Mater Biol Appl*, 60:374-83. DOI 10.1016/j.msec.2015.11.064.
15. Wu YH, Chiu YC, Lin YH, *et al.*, 2019, 3D-printed Bioactive Calcium Silicate/Poly-ε-caprolactone Bioscaffolds Modified with Biomimetic Extracellular Matrices for Bone Regeneration. *Int J Mol Sci*, 20:942. DOI 10.3390/ijms20040942.
16. Ma H, Feng C, Chang J, *et al.*, 2018, 3D-printed Bioceramic Scaffolds: From Bone Tissue Engineering to Tumor Therapy. *Acta Biomater*, 79:37-59. DOI 10.1016/j.actbio.2018.08.026.
17. Carlisle EM, 1970, Silicon: A Possible Factor in Bone Calcification. *Science*, 167:279-80.
18. Shie MY, Ding SJ, Chang HC, 2011, The Role of Silicon in Osteoblast-like Cell Proliferation and Apoptosis. *Acta Biomater*, 7:2604-14. DOI 10.1016/j.actbio.2011.02.023.
19. Chen YW, Ho CC, Huang TH, *et al.*, 2016, The Ionic Products from Mineral Trioxide Aggregate-induced Odontogenic Differentiation of Dental Pulp Cells via Activation of the Wnt/β-catenin Signaling Pathway. *J Endod*, 42:1062-9. DOI 10.1016/j.joen.2016.04.019.
20. Ge L, Li QL, Huang Y, *et al.*, 2014, Polydopamine-coated Paper-stack Nanofibrous Membranes Enhancing Adipose

- Stem Cells' Adhesion and Osteogenic Differentiation. *J Mater Chem B*, 2:6917-23. DOI 10.1039/c4tb00570h.
21. Ku SH, Ryu J, Hong SK, *et al.*, 2010, General Functionalization Route for Cell Adhesion on Non-wetting Surfaces. *Biomaterials*, 31:2535-41. DOI 10.1016/j.biomaterials.2009.12.020.
 22. Lee YB, Shin YM, Kim EM, *et al.*, 2016, Mussel Adhesive Protein Inspired Coatings on Temperature-responsive Hydrogels for Cell Sheet Engineering. *J Mater Chem B*, 4:6012-22. DOI 10.1039/c6tb01057a.
 23. Rim NG, Kim SJ, Shin YM, *et al.*, 2012, Mussel-inspired Surface Modification of Poly(L-lactide) Electrospun Fibers for Modulation of Osteogenic Differentiation of Human Mesenchymal Stem Cells. *Colloids Surf B*, 91:189-97. DOI 10.1016/j.colsurfb.2011.10.057.
 24. Sun X, Cheng L, Zhao J, *et al.*, 2014, bFGF-grafted Electrospun Fibrous Scaffolds via Poly(dopamine) for Skin Wound Healing. *J Mater Chem B*, 2:3636-45. DOI 10.1039/c3tb21814g.
 25. Lee H, Rho J, Messersmith PB, 2009, Facile Conjugation of Biomolecules Onto Surfaces via Mussel Adhesive Protein Inspired Coatings. *Adv Mater*, 21:431-4. DOI 10.1002/adma.200801222.
 26. Jo S, Kang SM, Park SA, *et al.*, 2013, Enhanced Adhesion of Preosteoblasts Inside 3D PCL Scaffolds by Polydopamine Coating and Mineralization. *Macromol Biosci*, 13:1389-95. DOI 10.1002/mabi.201300203.
 27. Chen X, Wu Y, Ranjan VD, *et al.*, 2018, Three-dimensional Electrical Conductive Scaffold from Biomaterial-based Carbon Microfiber Sponge with Bioinspired Coating for Cell Proliferation and Differentiation. *Carbon*, 134:174-82. DOI 10.1016/j.carbon.2018.03.064.
 28. Shie MY, Chiang WH, Chen IWP, *et al.*, 2017, Synergistic Acceleration in the Osteogenic and Angiogenic Differentiation of Human Mesenchymal Stem Cells by Calcium Silicate-graphene Composites. *Mater Sci Eng C Mater Biol Appl*, 73:726-35. DOI 10.1016/j.msec.2019.01.059.
 29. Liu H, Li W, Luo B, *et al.*, 2017, Icaritin Immobilized Electrospinning Poly(l-lactide) Fibrous Membranes via Polydopamine Adhesive Coating with Enhanced Cytocompatibility and Osteogenic Activity. *Mater Sci Eng C Mater Biol Appl*, 79:399-409. DOI 10.1016/j.msec.2017.05.077.
 30. Shie MY, Ding SJ, 2013, Integrin Binding and MAPK Signal Pathways in Primary Cell Responses to Surface Chemistry of Calcium Silicate Cements. *Biomaterials*, 34:6589-606. DOI 10.1016/j.biomaterials.2013.05.075.
 31. Steeves AJ, Atwal A, Schock SC, *et al.*, 2016, Evaluation of the Direct Effects of Poly(dopamine) on the *in vitro* Response of Human Osteoblastic Cells. *J Mater Chem B*, 4:3145-56. DOI 10.1039/c5tb02510a.
 32. Liu H, Li W, Wen W, *et al.*, 2017, Mechanical Properties and Osteogenic Activity of Poly(l-lactide) Fibrous Membrane Synergistically Enhanced by Chitosan Nanofibers and Polydopamine Layer. *Mater Sci Eng C Mater Biol Appl*, 81:280-90. DOI 10.1016/j.msec.2017.08.010.
 33. Lee YB, Shin YM, Lee JH, *et al.*, 2012, Polydopamine-mediated Immobilization of Multiple Bioactive Molecules for the Development of Functional Vascular Graft Materials. *Biomaterials*, 33:8343-52. DOI 10.1016/j.biomaterials.2012.08.011.
 34. Tsai CH, Hung CH, Kuo CN, *et al.*, 2019, Improved Bioactivity of 3D Printed Porous Titanium Alloy Scaffold with Chitosan/Magnesium-calcium Silicate Composite for Orthopaedic Applications. *Materials*, 12:203. DOI 10.3390/ma12020203.
 35. Kao CT, Chen YJ, Ng HY, *et al.*, 2018, Surface Modification of Calcium Silicate via Mussel-inspired Polydopamine and Effective Adsorption of Extracellular Matrix to Promote Osteogenesis Differentiation for Bone Tissue Engineering. *Materials*, 11:1664. DOI 10.3390/ma11091664.
 36. Wu C, Zhou YZ, Lin C, *et al.*, 2012, Strontium-containing Mesoporous Bioactive Glass Scaffolds with Improved Osteogenic/Cementogenic Differentiation of Periodontal Ligament Cells for Periodontal Tissue Engineering. *Acta Biomater*, 8:3805-15. DOI 10.1016/j.actbio.2012.06.023.
 37. Chen YW, Yeh CH, Shie MY, 2015, Stimulatory Effects of the Fast Setting and Degradable Ca-Si-Mg Cement on Both Cementogenesis and Angiogenesis Differentiation of Human Periodontal Ligament Cells. *J Mater Chem B*, 3:7099-108. DOI 10.1039/c5tb00713e.
 38. Chou MY, Kao CT, Hung CJ, *et al.*, 2014, Role of the p38 Pathway in Calcium Silicate Cement-induced Cell Viability and Angiogenesis-related Proteins of Human Dental Pulp Cell *in vitro*. *J Endod*, 40:818-24. DOI 10.1016/j.joen.2013.09.041.
 39. Cheng CH, Chen YW, Lee KX, *et al.*, 2019, Development of Mussel-inspired 3D-printed Poly (lactic acid) Scaffold Grafted with Bone Morphogenetic Protein-2 for Stimulating Osteogenesis. *J Mater Sci Mater Med*, 30:78. DOI 10.1007/s10856-019-6279-x.
 40. Poh CK, Shi Z, Lim TY, *et al.*, 2010, The Effect of VEGF Functionalization of Titanium on Endothelial Cells *In vitro*. *Biomaterials*, 31:1578-85. DOI 10.1016/j.biomaterials.2009.11.042.